

INVESTIGATION OF FORESTS AS FACTOR OF AERODYNAMIC PROTECTION OF SETTLEMENTS FROM DUST STORMS AND INDUSTRIAL POLLUTION

Orlov S.A.*, Vasenin I.M. and Khmeleva M.G.

*Author for correspondence
Department of Applied Aerodynamics,
Tomsk State University,
Tomsk, 634045,
Russia
E-mail: orlov@ff.tsu.ru

ABSTRACT

The paper presents the results of the experimental research on the aerodynamic resistance forces of different types of the forest plantations and the types of tree planting under the air mass motion. The results of mathematical modeling of moving a dust cloud filled with different sized particles in a forest massif are shown with account of sizes and the mass of the crown elements, the resistance forces of separate elements of tree crowns. While investigating branch resistances as dimensionless parameters one can separate the two Reynolds numbers: one of them is calculated by the diameter of a needle, the other by the diameter of a branch – base to which the needles are attached. As a method to determine the resistance forces of the treetops, in this paper a hydrodynamic approach is applied where the authors propose to investigate the resistance coefficient of the branch (being investigated) when it is moving in water. On this grounds in order to investigate the resistance coefficients of the woodland a setting was assembled, it was based on the study of falling these elements into a transparent pool of water under the action of gravity produced by special cargoes. It was revealed that the resistance coefficient of the conifer crowns greatly depends on the velocity of a climbing stream. Thus, at high Reynolds numbers a well-known effect of "folding" of the crown elements is observed and the resistance coefficient of the whole crown tends to the resistance coefficient of the needleless branches. With the flows up to 20 m/s the main parameter which determines the flow past the bodies with the predetermined geometry is the Reynolds number. On the basis of the data obtained from the experiment a mathematical modeling of a dust cloud was carried out in a stand of forest. The propagation of the wind in the stand of forest is described by three-dimensional equations of gas dynamics. To describe the dust cloud the continuum model consisting of dust particles was adopted as a mathematical model. It takes into account the forces acting on the particles from the air, as well as the sizes of dust particles and the

change of momentum of particles in collisions with the elements of trees. In this case it is assumed that in such collisions a dust mass falls on the trees and it is proportional to the surface of these elements, to the dust flow on them and to a certain coefficient of the particle capture which can vary from zero to unity. The simulation of the dust particles is based on the Eulerian approach, the movement of the mass is modeled in the volume. The influence of different types of forests and forms of the forest plantations on the process of distribution of the dust cloud of particles was also investigated. To protect from a dust cloud a series of computational experiments of comparing the efficiency of certain variants of the forest protection zones has been carried out. The results can be used while designing the measures to protect the settlements from the harmful ejections and emissions of the industrial enterprises. In this paper the results of the parametric investigation for different types of particles have been presented, the conclusions as regards the efficiency of some types of the forest protecting belts have been made. The problem of modeling the distribution of the dust cloud with the account of the viscosity forces recorded in the approximation of the boundary layer in the forest belt has been solved.

INTRODUCTION

Urbanization, growth of the industrial production and the development of large urban agglomerations result in exacerbation of the problem of clean air and protection of the populated areas from harmful industrial emissions. One of the ways to be protected from such phenomena is to create barrage forest bands, massifs and plantations on the way to possible spreading of the technological emissions, dust clouds produced by industrial enterprises, harmful emissions of the road transport. There is a great number of researches on the problem of flows in the permeable barriers of different nature. They are the experimental papers [1,2] in which the authors described detailed investigations of permeability of a model vegetation cover as well as papers [3,4] in which the authors give the solutions of such

problems by means of the methods of mathematical modeling [3,4].

The use of the systems of forest protective bands is known for a long time. However by now the information allowing to model their influence on the motion of air masses is insufficient. The developed numerical methods to compute the propagation of wind gusts in the forest massifs require specifying of the resistance coefficients in the elements of the forest massifs. In view of the shortage of the concrete data on these coefficients there arose a necessity to carry out the experimental work on their definitions in order to apply them later in the numerical simulations.

While investigating the propagation of the air masses in the forest massifs a decisive role is played by the force interaction of the air stream and the elements of the forests.

FORMULATION OF THE PROBLEM

The motion of the air masses in a forest massif is described by the unsteady-state three-dimensional integral equations which in the volume Ω with the surface S and the account of porosity ξ is written in [5]:

$$\left\{ \begin{array}{l} \frac{\partial}{\partial t} \int_{\Omega} \rho \xi d\Omega + \int_S \rho (\vec{U} \cdot \vec{n}) ds = \dots \\ \frac{\partial}{\partial t} \int_{\Omega} \rho \xi \vec{U} d\Omega + \int_S \rho \xi (\vec{U} \cdot \vec{n}) ds = \dots \\ \frac{\partial}{\partial t} \int_{\Omega} \rho \xi \left(e + \frac{|\vec{U}|^2}{2} \right) d\Omega + \int_S \rho \xi \left(\vec{U} \cdot \vec{n} \right) \left(e + \frac{|\vec{U}|^2}{2} + \frac{p}{\rho} \right) ds = 0, \end{array} \right. \quad (1)$$

where t – the time; p – the pressure; ρ – the density; e – the internal energy; \vec{U} – the the speed vector of the air; \vec{n} – the unit normal to the boundary S ; the operator $(\vec{U} \cdot \vec{n})$ – is the projection of \vec{U} on the normal \vec{n} , \vec{F} – the resistance force of forest massif elements.

The distribution of air masses in the forest massifs is influenced by the intensity of interaction between the elements of the tree crowns and the air. In view of the fact that in the forest there is a spectrum of the characteristic dimensions of the solid phase - from the trunks with a characteristic size of about a meter to the needles with the size about a millimeter, then the dependence of the effective force of the interfacial friction may possess a complicated structure.

For a comparative evaluation and determining the flow regime around the crown and the tree trunks it is necessary to take the average rate of the air mass $U \sim 10$ m / s , the air density $\rho_B \sim 1$ kg/m³, the air viscosity $\eta \sim 1.8 \cdot 10^{-5}$ Pa • s . With these parameters the Reynolds number of flowing around separate needles of the coniferous species is of the order $\sim 5 \cdot 10^2$. While flowing around the trunks, large branches and leaves the Reynolds number exceeds the critical value and the flow around these elements occurs in the turbulent regime. The resistance force exerted on individual tree trunks may be evaluated by applying the familiar relationships for the resistance coefficients of a circular cylinder [6].

The resistance force of individual needles of the coniferous trees can also be assessed as a resistance force of cylinders. However, in dense crowns the processes of flowing around individual needles influence each other. Therefore the resistance force of the branch needles is not

equal to the sum of the resistance forces of single needles and it should be evaluated as a force acting on a branch as a whole.

In this paper the experimental studies were carried out with the branches of a cedar pine and a spruce. While investigating the branch resistance one can separate the two Reynolds numbers: one of them is calculated by needles diameter, the other – by the diameter of the branch – base to which the needles are attached. However, the preliminary experiments showed that at the wind speeds up to 20 m / s the needle resistance forces are many orders of magnitude higher than the resistance of the branch to which the needles are attached. Therefore later the resistance forces were examined depending only on the Reynolds number calculated by the diameter of the needles.

One can assume that the resistance force per unit volume of the crown F (from equation 1) is proportional to the branch mass in this volume. For the most abundant tree species the masses and dimensions of the crowns were extensively investigated by biologists. Therefore, bearing in mind the application of the research results to calculate the forces \vec{F} – the resistance force of the branch was studied in the form:

$$f = \varphi(Re) m_d \frac{\rho_a U^2}{2} \quad (2)$$

where m_d – is the mass of the branch under study, $\varphi(Re)$ – the resistance coefficient. Then, knowing the function $\varphi(Re)$ one can calculate the resistance force \vec{F} using the formula

$$\vec{F} = \varphi(Re) M \frac{\rho_a U \cdot \vec{U}}{2} \quad (3)$$

where M – the branch mass per unit volume.

This expression denoting the resistance force of branches (3) differs from a more famous expression $\vec{F} = C_{RM} \frac{\rho_a U \cdot \vec{U}}{2}$ for the resistance forces. The point is that

according to the results of investigating the forest massifs, the crown mass of trees is well known but not the midsection S_M . At the same time, in using the experiments described below it is possible to determine the value $\varphi(Re)$ which has the form $\varphi_R = \frac{C_{RM} S_M}{m_d}$. Thus, the value $\varphi(Re)$ is

proportional to S_M . However, in the formula $\vec{F} = C_{RM} \frac{\rho_a U \cdot \vec{U}}{2}$ one should know the product $C_{RM} S_M$, but not each of the factors separately. This product is equal to $\varphi_R m_d$, which is used in simulation.

EXPERIMENTAL METHOD

In this paper a hydrodynamic approach is applied as a method to determine the function $\varphi(Re)$, when it is necessary to study the resistance coefficient of the branch when it is moving in water.

The main parameter determining the flow past the bodies of the preset geometry is the Reynolds number for the flows up to 20 m/s. Assuming the Reynolds number in the air and water to be equal we obtain relation (4):

$$\frac{U_a}{U} = \frac{\rho}{\rho_a} \frac{\eta_a}{\eta} \quad (4)$$

Here ρ , U , η are the density, the speed, and the dynamic viscosity of the air, ρ_B , U_B , η_B are the density, the speed and the dynamic viscosity of water. By substituting the familiar values of density, speed and the dynamic viscosity in (4) we obtain the speed ratios $U_a/U=0.056$.

Thus, to obtain the same Reynolds numbers in water which are achieved in the air stream, it is necessary to provide the flow rate almost 20 times smaller than in the air. When considering the air flow speed up to 20 m/s, in water the same Reynolds numbers are achieved at the speeds not exceeding 1.1 m/s.

Relying on this knowledge an installation based on the study of falling these elements in water has been constructed to investigate the resistance coefficients of the forest massif elements; it was based on the comprehensive study of these elements falling into a transparent pool of water under the action of gravity forces induced by special cargoes. A scheme of the assembled experimental setup is shown in Fig. 1.

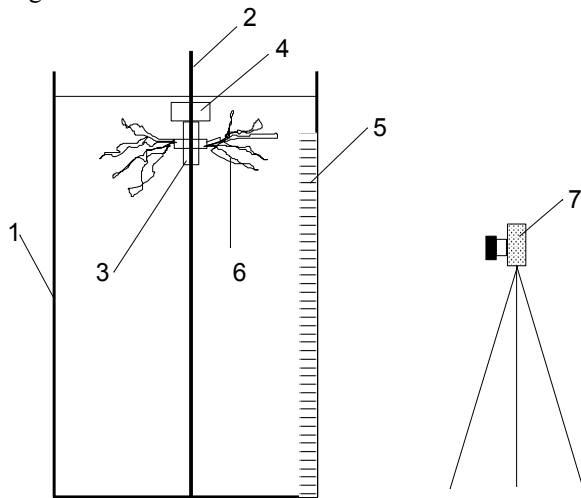


Figure 1 The scheme of the experimental installation

The following notations are given on the scheme: 1 – the transparent basin of water, its depth is 85 cm; 2 – a metallic core along which an element of the forest massif moves, being fixed to a sliding holder; 3 – a sliding holder; 4 – the load which causes the motion of the branch; 5 – the dimensional ruler to record the process of the fall; 6 – the element of the forest massif under investigation; 7 – the high-speed digital video camera Citius Imagine to register the falling process.

The force of gravity, the resistance force and the Archimedes force act on all the elements. The following notations are introduced: m_d – the mass of an element under investigation, m – the total weight of the cargo and the holder, U – the falling speed, ρ_m – the density of the material (the cargo is made of), ρ_d – the density of the element under investigation, x – the depth of submerging.

Due to the fact that all the branches have a complex structure including the needles, the problem to determine the density of branches becomes difficult; therefore it becomes possible to substitute the necessary branch density by the buoyant force value. Some added water mass m_{np} which must be taken into account is also involved in the motion process.

Then the motion of the system on the immersion is described by equations (5)-(6):

$$(m + m_d + m_{np}) \frac{dU}{dt} = (m + m_d)g - F_A - F_{Am} - (\varphi_R m_d + \varphi_{Rm}) \frac{\rho_g U^2}{2} \quad (5)$$

$$\frac{dx}{dt} = U \quad (6)$$

where φ_R – the resistance coefficient of the branches with the mass m_d , φ_{Rm} – the resistance coefficient of the cargo and the cargo holder, F_A – the buoyancy force of the branches, F_{Am} – the buoyancy force of the holder and the cargo.

The buoyancy forces for the holder and the branches were determined experimentally by selecting such a mass of the cargo in which the Archimedes force would be compensated by the force of gravity. This condition follows from (5) if it is assumed that the speed $U = 0$ at any time. Having found such a mass of the cargo the buoyancy forces were recorded and used in the subsequent calculations.

RESULTS OF EXPERIMENTS

The experimental conditions made it possible to carry out the investigation in a pond filled with water under the normal conditions. The pool depth was 85 cm, there were graduation lines in every 5 cm; they were used to measure the time spent by the tool holder on the passage. The videography was carried out at the speed of 800 frames per second. The pine branches were used in the experiment. Their mass was 37.13 g (the needle mass was 28.91 g, the needles mass fraction was 77.86 %, the average weight of one needle was 0.030, the number of needles was 1300 pieces, the average diameter of one needle was about 1 mm) and also the spruce branches (their mass was 27.101 g, the needle mass was 17.02 g, the mass share of needles was 62.8%), the average weight of one needle was 0.0057 g. The number of needles on the branches was about 3,000 units, the average diameter of a needle was about 1 mm).

It was found that the speed of the holder with the load and branches reached a steady motion regime when it was passing the mark of 20 cm, further the fall occurred at a constant speed. This fact allows one not to consider the added water mass but (knowing the resistance coefficients of the holder and the cargoes) to calculate the resistance of branches using equation (5) and supposing that the speed is constant and equal to the stationary one in the points where it reached a steady value. The equation for the resistance coefficient will take on the form:

$$\varphi_R = 2 \frac{[(m + m_d)g - F_A - F_{Am}]}{\rho_g U^2 m_d} - \frac{\varphi_{Rm}}{m_d} \quad (7)$$

As a result of a series of experiments the values of average stationary speeds of the holder with the cedar and pine branches were obtained as well as the resistance coefficients of the cedar and pine branches as a function of the Reynolds number. On the basis of the obtained results the dispersion and regression analyses were carried out and as a result the dependences of the resistance coefficient for the unit volume of the cedar pine and the spruce crowns were received (8) and (9).

$$\varphi_R(\text{Re}) = \exp(1,4868 - 0,0067 \cdot \text{Re} + 4,2260 \cdot 10^{-6} \cdot \text{Re}^2 + 2,2288 \cdot 10^{-9} \cdot \text{Re}^3 - 4,5611 \cdot 10^{-12} \cdot \text{Re}^4 + 1,6816 \cdot 10^{-15} \cdot \text{Re}^5) \quad (8)$$

$$\varphi_R(\text{Re}) = \exp(1,0804 - 0,00058 \cdot \text{Re} - 7,1077 \cdot 10^{-6} \cdot \text{Re}^2 + 1,0238 \cdot 10^{-8} \cdot \text{Re}^3 - 5,4898 \cdot 10^{-12} \cdot \text{Re}^4 + 1,1099 \cdot 10^{-15} \cdot \text{Re}^5) \quad (9)$$

Figure 1 presents the obtained dependences and the experimental points for the resistance coefficients of a cedar pine unit volume (Fig. 1a) and the spruce volume unit (Fig. 1b). Figure 1 presents the additional experimental points denoted by crosses which characterize the resistance coefficient of the branches without needles. It was found out that the resistance coefficient of the coniferous tree crowns is strongly dependent on the speed of the climbing stream. Thus, at high Reynolds numbers one can observe a well-known effect of "folding" the crown elements and the resistance coefficient of the whole crown tends to the resistance coefficient of the needleless branches.

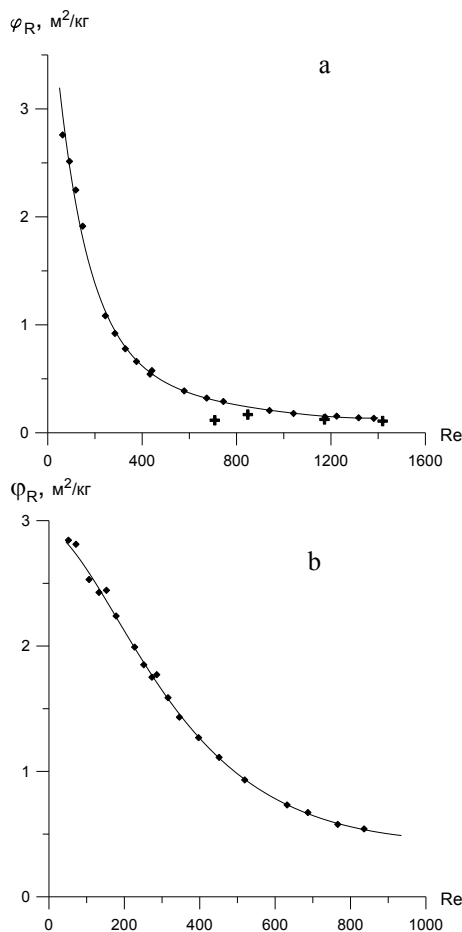


Figure 1 The resistance coefficient of a unit volume of the cedar pine (a) and the pine (b) depending on the Reynolds number

MATHEMATICAL MODELLING OF A DUST CLOUD MOTION

The wind distribution in the forest massif is described by three-dimensional gas dynamics equations (1). The influence of the forest on the air motion is allowed for by the gas dynamics equations (1). The influence of forest on the air movement is allowed for by the porosity functions ξ and the force interaction F . In assuming a small mass concentration of dust in the air masses its influence on the motion of the air masses is neglected. The interaction of air with the treetops is modeled by (3) which includes the coefficient of resistance per unit volume of the tree crown.

The important geometric parameters affecting the tree aerodynamics are: the tree height, the height and the diameter of the crown, the average diameter of the barrel,

the average number and the diameter of the tree branches, the shape of the crown. In the mathematical three-dimensional model the crown shape was taken to be axisymmetric. For firs and cedars this shape was taken to be cone shaped.

The tree is modeled to be a porous structure consisting of two volumes. One volume is a circular cone of h height with the basis radius R . The basis of the cone is located at the altitude of $H-h$ where H is the height of the spruce. Since in the model the viscosity affects the flow only by means of the forces of resistance to the porous structure then in order to take account of the resistance forces of the trunk the latter was assumed to be porous. In this case the porosity parameters of the trunk were chosen so that the resulting resistance force of the trunk was equal to the experimental resistance force of the cylinder having the diameter equal to the average diameter of the barrel. The dependences concerning the needle mass content in one hectare of vegetation were taken from [4] and, basing on this information, the crown mass of one simulated tree was calculated. Later the resulting calculations were confirmed by the investigations dealing with the characteristic properties of biomass formation of cedar pine crowns described in works [7, 8].

A continuum model consisting of the dust cloud is adopted as a mathematical model to describe the dust cloud. In this case the forces acting on the dust particles on the part of air are taken into account as well as the size of dust particles and the changes in the particles momentum in collisions with the tree elements. Thus, it is assumed that in such collisions a great amount of dust is deposited on trees, its mass is proportional to the surface of these elements, to the dust flow on them and to a certain coefficient of the particles capture K_p which can vary from zero to unity. At the same time it is assumed that the particles completely lose their momentum during the collisions with the elements of the forest massif.

Under the above assumptions the integral equations of mass and momentum conservation of a dust cloud have the form (10) - (11):

$$\frac{\partial}{\partial t} \int_{\Omega} \xi \rho_s d\Omega + \int_{\Omega} \xi \rho_s (\vec{U}_s \cdot \vec{r}) - \int_{\Omega} \rho_s (1 - \xi) \rho_s |\vec{U}_s| u_{de} \quad (10)$$

$$\frac{\partial}{\partial t} \int_{\Omega} \rho_s \xi \vec{U}_s u_{de} + \int_{\Omega} (\vec{U}_s \cdot \vec{r}) \rho_s - \int_{\Omega} \frac{\rho_s}{m_s} \vec{r} u_{de} - \int_{\Omega} (1 - \xi) \rho_s |\vec{U}_s| u_{de} - \int_{\Omega} \rho_s \vec{g} \cdot \vec{r} \quad (11)$$

where ρ_s - the density of the dust cloud, \vec{U}_s - the vector of a particle speed, m_s - the mass of one particle, $\vec{f}_s = S_m C_R (\vec{U} - \vec{U}_s)$ - the force the air acts on a particle with, S_m - the midships area of a particle, C_R - the resistance coefficient, \vec{g} - the acceleration of gravity, K_p - the coefficient of the particle deposition on the crowns.

The resistance coefficient C_R determines the force of interacting the particles with the air flow, it is found by the formula:

$$C_R = \frac{24}{Re} (1 + 0,197 Re^{0,63} + 2,6 \cdot 10^{-4} Re^{1,38}) \quad (12)$$

where Re is the Reynolds number.

The solution of the systems of integral equations is carried out by the finite volume method. The computational domain is represented by a fixed set of equal finite volumes not

intersecting each other so that each node of the computational grid is contained in one volume. The values of the speed components of the gas motion as well as the gas parameters on the faces of the finite volumes are determined by applying the procedure of the rupture decay. The dust particle simulation is based on the Eulerian approach: the motion of the mass particles is modelled in the volume. To solve the equations of dust particle motion (10) - (11) the method of finite volumes is applied. An upstream recording of the speed differences is applied on the faces.

In this paper the spread of a dust cloud of a given volume is modelled under a wind gust within the region of X meters long, Y meters wide and Z meters high, where there is a porous barrier like a forest protection belt. The forest protection belt consists of several rows of trees and also has the symmetry planes. A simulation in the computational domain (which is X = 200 m long, Y = 5 m wide, Z = 50 m high) is discussed.

As the boundary conditions for the equations of the dust motion (10-11) the two forces are specified on the left boundary of the computational domain, the constant speed $U_0=10$ m/s operating throughout all the computation period from its beginning and a starting speed of settling the particles W_0 , the latter is due to the attraction force acting on the particles.

The condition of non-leaking through was specified on the symmetry planes so that the particles reaching the front ($y = 0$) and back ($y = Y$) boundaries of the computational domain do not leave it. The particles can freely penetrate through the upper boundary of the computational domain without changing the speed. The particles reaching the lower boundary of the computational domain are considered to have settled and are not involved into the further motion of the dust.

Since the air flows are of the turbulent character in the lower layers of the atmosphere, then it is necessary to take account of these phenomena.

The model from [1] is used as a parameter of the mixing method:

$$L = \frac{\kappa z}{1 + 2,5z\sqrt{\frac{c_d s}{h}}} \quad (13)$$

where $c_d=0.03$, s – the specific density of the surface which characterizes the surface area of the vegetation elements per unit volume, h – the vegetation height .

Taking account of the resistance of the forest massif trees and the presence of viscosity the equations of the gas motion in the differential form are written in the form of (14). The turbulent viscosity forces are taken into account in the boundary layer approximation.

$$\begin{cases} \frac{\partial U}{\partial t} + U \frac{\partial U}{\partial x} + V \frac{\partial V}{\partial y} + W \frac{\partial W}{\partial z} = -\frac{1}{\rho} \frac{\partial p}{\partial x} - \frac{F}{\rho} + \frac{\partial}{\partial z} \left[(\varepsilon + \nu) \frac{\partial U}{\partial z} \right], \\ \frac{\partial V}{\partial t} + U \frac{\partial U}{\partial x} + V \frac{\partial V}{\partial y} + W \frac{\partial W}{\partial z} = -\frac{1}{\rho} \frac{\partial p}{\partial y} - \frac{F}{\rho}, \\ \frac{\partial W}{\partial t} + U \frac{\partial U}{\partial x} + V \frac{\partial V}{\partial y} + W \frac{\partial W}{\partial z} = -\frac{1}{\rho} \frac{\partial p}{\partial z} - \frac{F}{\rho}, \\ \frac{\partial \rho}{\partial t} + \frac{\partial(\rho U)}{\partial x} + \frac{\partial(\rho V)}{\partial y} + \frac{\partial(\rho W)}{\partial z} = 0, \end{cases} \quad (14)$$

While simulating the rectangular area with the distances along three directions X, Y, Z, and the space steps dx , dy , dz was considered. The coordinate origin is placed in the left ($x = 0$) low ($y = 0$) near ($z = 0$) angle. The boundary

conditions with the account of the plantation symmetry are written down in the form:

$$\begin{aligned} U|_{x=0} = U_0(z), \quad V|_{x=0} = 0, \quad W|_{x=0} = 0; \quad \frac{\partial U}{\partial x}|_{x=X} = 0, \quad \frac{\partial V}{\partial x}|_{x=X} = 0, \quad \frac{\partial W}{\partial x}|_{x=X} = 0; \\ \frac{\partial U}{\partial y}|_{y=0} = 0, \quad V|_{y=0} = 0, \quad \frac{\partial W}{\partial y}|_{y=0} = 0; \quad \frac{\partial U}{\partial y}|_{y=Y} = 0, \quad V|_{y=Y} = 0, \quad \frac{\partial W}{\partial y}|_{y=Y} = 0; \quad (15) \\ U|_{z=0} = 0, \quad V|_{z=0} = 0, \quad W|_{z=0} = 0; \quad \frac{\partial U}{\partial z}|_{z=Z} = 0, \quad \frac{\partial V}{\partial z}|_{z=Z} = 0, \quad \frac{\partial W}{\partial z}|_{z=Z} = 0; \end{aligned}$$

The uniform distribution of the normal pressure and density over the entire volume $p|_{t=0} = 10^5$ Pa, the initial density of air $\rho|_{t=0} = 1,29$ kg/m³ were supposed to be the initial conditions. The initial profiles $U_0(z)$ on the left boundary were taken from the experimental data for the developed turbulent boundary layer in the atmosphere. The speed profile $U_0(z)$ was chosen so that the speed was equal to 10 m/s in the region above the forest massif and the profile corresponded to the experimental data at the trees altitude and lower.

As a result of modelling the effects of different types of the forest planting and the forms of tree plantations on the process of propagating the dust cloud particles of different sizes (0.1 mm, 0.2 mm, 0.3 mm, 0.4 mm, 0.5 mm) have been investigated.

Fig. 3 presents the distribution of the particle masses in the middle section of the forest band with a row tree planting and the undergrowth after 5 seconds after the beginning of a wind gust.

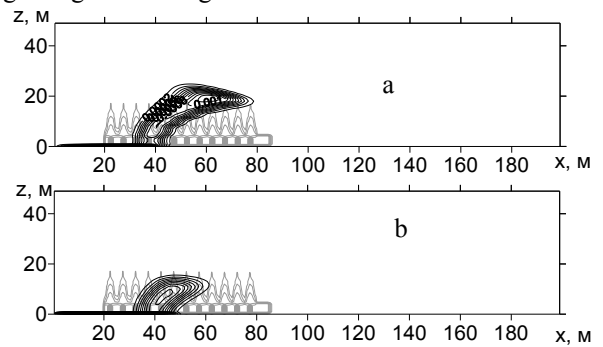


Figure 3 The distribution of the particle mass in middle section of the forest band with a row planting of trees and the undergrowth at the time moment $t = 5$ seconds, a) the particles 0.1 mm in size, b) the particles 0.5 mm in size.

It should be noted that there is practically no particle motion under the tree crowns. Large particles penetrate into the area of the undergrowth and the tree crowns, lose their speed and settle either on the ground or the tree crowns. At the same time the most part of the retarded particles settle on the first three trees of the forest band section. Further the particles penetrate inside along the forest band to a less degree and only small ones (0.1 mm) may find themselves in the far zones of the forest band with the undergrowth because they rise high and settle down from above.

Figure 4 presents the distribution of the mass of small particles in the fir forest band with a straight row plantation consisting of 12 trees with the undergrowth and without the latter during 10 seconds after beginning of the dust cloud motion. In the figure one can see that in the absence of the undergrowth the lower part of the dust cloud freely penetrates along the direction of the wind motion, i.e. the space under trees is practically blown through. At the same

time the presence of the undergrowth practically prevents the penetration of the particles from the lower part of the dust cloud into the zone behind the forest band. One should note the presence of a part of particles which fly above the forest-protecting band and continue moving behind the last tree. However, in this region the distribution of the longitudinal speed component is much lower as compared with the left part of the calculation region, which leads practically to the slow deposition of the dust particles on the Earth surface.

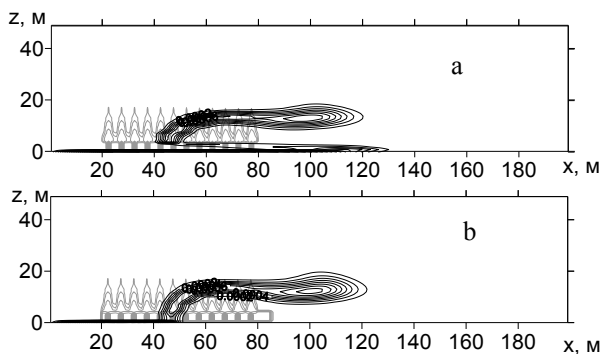


Figure 4 The distribution of the particle mass 0.1 mm in size at the time moment $t = 10$ sec in the middle section of the forest band with the row tree planting a) without the undergrowth, b) with the undergrowth.

Fig. 5 illustrates the distribution of the particles settling on the Earth along the calculation region with the row tree planting without the undergrowth and with a staggered planting of trees without the undergrowth.

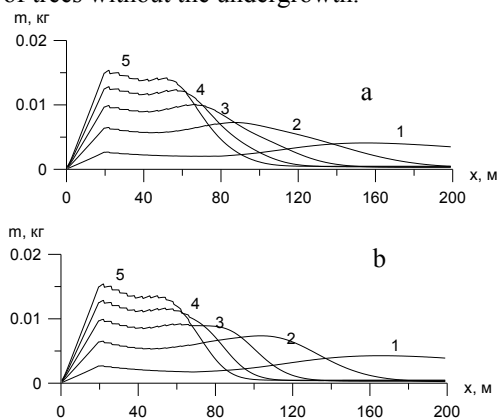


Figure 5 The distribution of the particles settled on the ground along the calculation region a) with a row planting of trees without the undergrowth, b) with a staggered planting of trees without the undergrowth. (1 – $d_s=0,1$ mm; 2 – $d_s=0,2$ mm; 3 – $d_s=0,3$ mm; 4 – $d_s=0,4$ mm; 5 – $d_s=0,5$ mm)

It can be noted that a greater part of particles with the sizes of 0.3 mm, 0.4 mm, 0.5 mm settle down at the very beginning of the calculation zone, and a maximum of the settled mass of particles is achieved in the zone where one can observe the dust cloud penetration into the area of the first tree. A greater part of particles of a relatively large sizes settles down here. The particles of 0.1 mm and 0.2 mm in size settle down in the second part of the modeled area which is caused by their smaller sizes and, as a consequence, by the opportunity to fly a greater distance near the earth surface circling the tree trunks, where there are no crowns.

The character of dependences for different variants of tree planting is similar and the differences are insignificant. It is worthwhile mentioning a toothed character of the dependences in the range from 20 to 80 meters. This is due to the presence of the tree trunks in the zone where there is a dip of the mass of the deposited particles. Since the figure presents the integral characteristic of the mass of the particles deposited on the width of the modeled area and the particles in the process of dissemination fly around the trees trunks not penetrating inside them; in the sections coinciding with the tree trunks one can observe a sharp drop in mass. Small peaks in front of the tree trunks are associated with this fact and conversely the decrease in the mass of particles behind the trunks. A certain part of particles does not fly around the tree trunks and lingers in front of them.

A somewhat different picture is observed in Fig. 6 which shows the distribution of particles deposited on the ground in the forest underbrush with an ordinary tree planting and a staggered pattern. In order not to cram the figures with details for small particles (0.1 mm and 0.2 mm) and for large ones (0.3 mm, 0.4 mm, 0.5 mm) only the dependences for 0.1 mm and 0.5 mm were taken.

It is worthwhile noting that in the presence of the undergrowth (as it was shown above) the lower portion of the dust cloud does not fly far along the forest band but is delayed among the first trees. Since one of the basic characteristics of the windbreaks is the mass fraction of particles overcoming the obstacle in a form of forest plantations, therefore the authors of this investigation compare the mass fraction of particles which reached the right boundary of the computational domain with different locations of the forest bands.

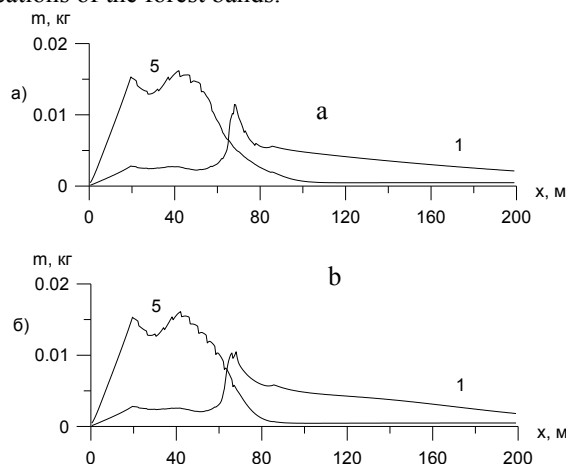


Figure 6 The distribution of particles deposited on the ground along the length of the computational domain, a) with the ordinary tree planting and the undergrowth, b) with the chess pattern of planting trees and the undergrowth. (1 – $d_s=0,1$ mm; 2 – $d_s=0,5$ mm)

It was found that the highly effective way to reduce the proportion of particles which reach the end of the computational domain is the forest shelter belt with a chess way of planting trees which, as compared with the row planting, makes it possible to reduce the share of small particles overcoming the forest area by 10%. The availability of the undergrowth with different ways of the tree planting reduces the share of traversing the small sized particles by 20% and big ones by 1.5%. The availability of

the forest band even with a denser tree planting (a row planting) reduces the share of traversing 0.1 mm sized particles by 15% and almost does not stop larger ones. Thus, it should be noted that the forest protection band reveals the highest efficiency while protecting from small sized dust (0.1 mm in size).

In the course of the computational experiments the authors investigated the speed distribution of the air flows passing through a permeable barrier in the form of a forest massif with account of addition of the viscosity term to the equations. The effect of accounting for the border layer on the motion of the dust particles of various sizes (from 0.1 mm to 0.5 mm) was also studied.

As a characteristic which was used to estimate the obtained speed profiles a dimensionless height is used as the height z referred to the tree height h as well as the dimensionless speed as the speed of the flow U divided by the speed of the airflow at the altitude of the tree tops U_h .

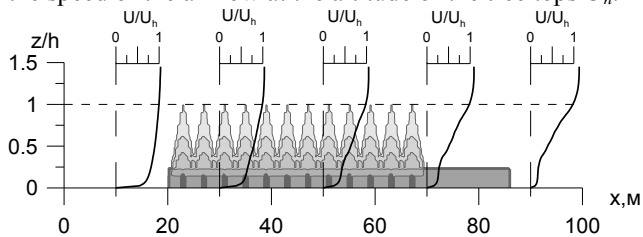


Figure 7 The computational domain with a set of the model trees and the undergrowth, the dimensionless speed profiles as a function of the dimensionless height obtained as a result of modeling in different sections.

As one can see in the Figure while going through the forest massif the speed profile is considerably influenced by the resistance force of the tree crowns as well as by the presence of the undergrowth. However, the reduction of speed in the near-ground region behind the undergrowth is very well noticeable in this Figure; the latter is due to the account of the viscosity term in the equation for motion. When the speed is decreased the profile speed in the near-ground region is somewhat smoothed out in the near-ground region which is also due to the viscosity term of the equation. This speed profile agrees rather well with the experimental data [3].

In the case of the forest band without the undergrowth the distribution of the speed profiles will somewhat be different due to the presence of the free zone between the earth surface and the lower part of the crowns. Fig. 8 presents this distribution of the profiles of the longitudinal speed.

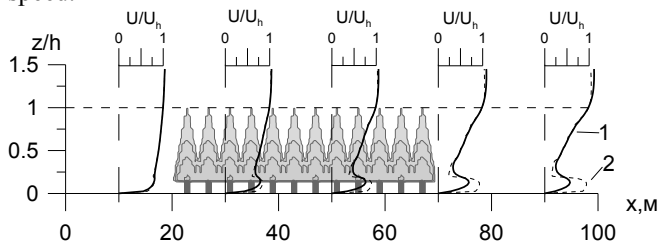


Figure 8 The computational domain with a set of sample trees without the undergrowth and dimensionless velocity profiles obtained from the simulation in different sections. (1 - including the turbulent boundary layer, 2 - excluding the turbulent boundary layer).

For every profile the solid line denotes the speeds obtained with account of the turbulent boundary layer, the dotted line – without account of the turbulent boundary layer.

This figure also shows the influence of the resistance force of the tree crowns and much more clearly one can see the impact of the viscosity term in the equation of motion. In the ground floor the velocity profile is significantly smoothed and the longitudinal speed in this area is reduced due to the turbulent mixing. As one can see the solid and dashed lines practically coincide in the upper part of the trees, indicating a stronger influence of the coefficient of resistance coefficient to the crown retention capacity of the forest. In the near-ground area it is the boundary layer that plays the most important part; the speed decreases at the expense of viscosity during the turbulent mixing of the air.

The distribution pattern of particles deposited on the ground has slightly changed. The proportion of fine particles (0.1 mm and 0.2 mm) deposited in the area lying immediately behind the forest belt significantly increased. This is associated with the reduction in the speed due to the turbulent mixing in the bottom of the dust cloud. The share of large particles deposited on the earth surface has changed very little as well as their distribution along the forest belt.

CONCLUSION

The following results have been obtained in this paper:

On the basis of the developed experimental methods in order to determine the resistance coefficients of the tree crowns the dependences of the resistance coefficients per unit mass of the spruce and cedar pine crowns were obtained depending on the Reynolds number within the range from 62 to 1381 for the spruce and from 53 to 935 for the cedar. It was shown that for coniferous trees at high speeds the effect of "folding" the elements of crowns is observed, and the resistance coefficient of the crowns tends to the resistance coefficient of the branches without needles.

A three-dimensional mathematical model of moving the air masses with different particle sizes in the space, with permeable windbreaks of different configurations, mass and geometrical characteristics has been constructed. In the process of simulation the authors used their own experimental data to assess the resistance forces of the tree crowns.

The results of moving a dust cloud in the region with the windbreaks have been obtained. The abilities for dust detention of various configurations have been assessed. It was found out that the forest shelter belt of trees planted in a staggered order is most effective in decreasing the particles which reach the end of the computational domain. The availability of the undergrowth with different variants of tree planting reduces the proportion of traversing the small-sized particles by 20%, the large ones - by 1.5%.

The problem of simulating the spread of the dust clouds with account of the viscosity forces recorded in the approximation of the boundary layer of the forest band has been solved. It was found out that in the near-ground region of the forest protecting band the wind speed lowers at the expense of the viscosity term in the motion equations. The dimensionless wind speed profiles were obtained in different sections of the forest protecting band. The results of the

calculations coincide with the experimental data known before.

It was revealed that in case of the forest bands with staggered and row plantings without the undergrowth a significant settling of fine particles (with the sizes 0.1 and 0.2 mm) in the area immediately behind the forest belt is associated with reducing the speed at the expense of the viscosity forces at the bottom of the dust cloud. By this fact a well-known phenomenon can be explained when sand and snow drifts are observed near the forest bands.

The simulation results were compared with the experimental data and a good coincidence of the results has been revealed.

ACKNOWLEDGEMENT

The reported study was supported by RFBR, research project No. 14-01-31327-мол_a.

REFERENCES

[1] Dubov A.S., Marunich L.P., Marunich S.B., Turbulence in the vegetation cover, *Gidrometeoizdat*, 1982, 184 p.

[2] Sergeev A.L., The ecological role of forest plantations in the accumulation and redistribution of heavy metals and radionuclides in soils of the northern forest, *Dissertation for PhD, Orel, Orel state agricultural university*, 2008, 176 p.

[3] Yevgeny A. Gayev, Julian C.R. Hunt., Flow and Transport Processes with Complex Obstructions, *NATO Science Series, Mathematics, Physics and Chemistry*, 2007, Vol.236, 414 p.

[4] Sitnik V.V. Modeling the influence of vegetation on the distribution of an array of acoustic disturbances, *Mathematic modeling*, Vol. 19, N 8, 2007, p.90-96.

[5] Godunov S.K., Zabrodin A.V., Kraiko A.N., Numerical solution of multidimensional problems of gas dynamics, *Moscow, Nauka*, 1976, 400 p.

[6] Handbook of heat exchangers. In two volumes., *Vol.1, Moscow, Energoatomizdat*, 1987, 561 p.

[7] Tretyakova V.A., Distribution of tree diameters in dense cultures of pine, spruce and cedar, *Lesovedenie*, 2005, N5, p.72-75.

[8] Tretyakova V.A., Differentiation and growth of tree crops major tree species in Siberia, *Dissertation for PhD, Krasnoyarsk, Institute of forest, Siberian department of Russian Scientific Academy*, 2006, 171 p.